Spectral DPCM for Lossless Compression of 3D Hyperspectral Sounding Data

JARNO MIELIKAINEN, OLGA KUBASOVA, PEKKA TOIVANEN
Department of Information Technology
Lappeenranta University of Technology
P.O. Box 20, 53850 Lappeenranta,
FINLAND

Abstract: - A spectral linear prediction compression scheme for lossless compression of hyperspectral images is proposed in this paper. Since hyperspectral images have a great deal of correlation from band to band, spectral linear prediction algorithm, which utilizes information from several bands, is very efficient for compression purposes. The proposed algorithm is compared to JPEG-LS and CALIC encoding schemes. All algorithms have been tested on 10 real 3D sounding images and their results in term of compression ratios are shown. Amount of compression obtained by the new algorithm is significantly higher compared to the previously proposed lossless compression methods for hyperspectral images.

Key-Words: - Hyperspectral images, Sounder images, Lossless compression, Image compression

1 Introduction

Lossless compression techniques, as their name implies, involve no loss of information [1]. Lossless compression is used for applications that cannot tolerate any differences between the original and reconstructed data, such as medical imaging, global water and energy cycle, the Earth and other planets observations, climate weather connection, improvements in weather prediction, trace gases, etc.

Recently hyperspectral images have been widely used in these applications in order to provide more precise and accurate information. National Ocean and Atmospheric Administration (NOAA) [2] and National Aeronautics and Space Administration (NASA) [3] involve 3D hyperspectral imaging data as well as 3D sounding data in their research.

Hyperspectral instruments such as Atmospheric Infrared Sounder (AIRS) [4], Cross-track Infrared Sounder (CrIS) [5], Interferometer Atmospheric Sounding Instrument (IASI) [6], Geosynchronous Imaging Fourier Transform Spectrometer (GIFTS) [7], and Hyperspectral Environmental Suite (HES) [8], and Airborne Visible/Infrared Imaging Spectrometer (AVIRIS) [9] daily generate large volumes of three-dimensional hyperspectral data.

Hyperspectral sounding data provides much more precise information about atmospheric temperature, moisture, clouds, aerosols and surface properties than hyperspectral imaging data, but storage and transition of these images demand much more resources. That is why compression algorithms must be developed.

Lossless compression algorithms, such as JPEG-LS [10], context-based adaptive lossless image coding (CALIC) [11] and specific gray scale satellite image compression methods [12], and which effectively compress 2D data, are not suitable for 3D data compression. They do not utilize the high correlation between disjoint bands in 3D image spectra. Recently their performance has been improved by involving reordering techniques, such as [13] and [14]. In Section 2 3D sounding data, which has been used in our experiments, is presented. Section 3 of the paper

provides brief overview of JPEG-LS and CALIC techniques improved by fast nearest neighbor reordering technique [13], and detail the proposed compression scheme. Section 4 discusses the results in terms of compression ratios obtained by each of the algorithms, which have been tested on the same dataset. Section 5 summarizes the paper.

2 Data

We have experimented with 3D sounding data, captured by AIRS. Each image has 2108 spectral bands, 135 scan lines containing 90 cross-track footprints per san line [4]; temporal and spectral resolutions is over one thousand infrared channels and with spectral widths on the order of 0.5 wave number.

The algorithm has been tested on ten granules, five daytime (DT) and five nighttime (NT), which have been chosen from different geographical regions of the Earth. Their locations, UTC times, and local time adjustments are listed in Table 1.

Table 1. Ten selected AIRS granules for hyperspectral sounding data compression studies. [15]

Granule №	Time	Location
9	00:53:31 UTC -12H	Pacific Ocean, DT
16	01:35:31 UTC +2 H	Europe, NT
60	05:59:31 UTC +7 H	Asia, DT
82	08:11:31 UTC -5 H	North America, NT
120	11:59:31 UTC -10H	Antarctica, NT
126	12:35:31 UTC -0 H	Africa, DT
129	12:53:31 UTC -2 H	Arctic, DT
151	15:05:31 UTC +11 H	Australia, NT
182	18:11:31 UTC +8 H	Asia, NT
193	19:17:31 UTC -7 H	North America, DT

The data is available at the Distributed Active Archive Center (DAAC) located at the NASA Goddard Earth Sciences Data and Information Services Center (GES DISC) in Greenbelt, Maryland, USA and at [15].

3 Compression Schemes

Efficient 3D compression algorithms exploit interpixel redundancy in every image dimension. Hyperspectral images have a great deal of correlation in spectral direction caused by the image properties. This fact is successfully used to predict each band based on the previous bands. Different encoding schemes are built under the assumption that it takes fewer bits to encode differences between the predicted and the current band value, instead of encoding the original band.

3.1 Improved JPEG-LS and CALIC

The following two algorithms have been adapted for 3D image compression by involving fast nearest neighbor reordering (FNNR) scheme [13]. Context-adaptive predictor-based encoders CALIC and JPEG-LS gain advantages of the prediction technique, which allows obtaining the current pixel value utilizing pixels from its causal neighborhood. Detailed description of the CALIC can be found in [11]. JPEG-LS is also based on the predictive coding technique, where main compression phases are: prediction, context modeling, error encoding, and run mode [10]. The algorithms performance has been improved by the data preprocessing FFNR technique. Main idea of the dimension-reduced FNNR scheme is to rearrange the more spectrally correlated channels in 3D images together.

3.1 Spectral linear prediction

Linear prediction predicts the value for the next sample and computes the difference between predicted value and the original value. This difference is usually small, so it can be encoded with less its than the original value.

The technique implies prediction of each image band by involving number of bands along the image spectra. Each pixel is predicted using information provided by pixels in the previous bands in the same spatial position. An estimate for each pixel value is computed in the following way:

$$p'_{x,y,z} = \left\lfloor \sum_{i=1}^{M} a_{z,i}\, p_{x,y,z-i} + 1/2, \right\rfloor \qquad (1)$$

where $p_{x,y,z}$ is the value of the pixel at band z in spatial location (x, y), $a_{z,i}$, $i = 1...M$ denote prediction coefficients, M is a number of the image bands involved in prediction.

For each band the linear prediction is computed in such a way that the prediction coefficients minimize the expected value of the squared error. In other words, we are optimizing (1) by minimizing $\sum_{x,y} (p'_{x,y,z} - p_{x,y,z})^2$ for band z.

The linear prediction procedure is illustrated in figure 1. P_z is a column vector than containts all the pixels in the band z and $A_z=[a_{z,1}\ a_{z,2}\ \ldots\ a_{z,M}]$. The prediction coefficients (A_z) are quantized to the 16-bit values using uniform quantization (Q_1). The predicted pixel values (P_z') are quantized (Q_2) to the nearest integer values. After linear prediction the resulting residual band (D_z) is entropy coded with a range coder [18]. Compared to an arithmetic coder the files are less than 0.01 larger in most cases, but the range coder is 2-4 times faster than the arithmetic coder [19]. Each band is also entropy coded without prediction, and if its size is smaller than it is with prediction, the band is stored without prediction. The residual bands are obtained as pixelwise difference between the original and the predicted bands.

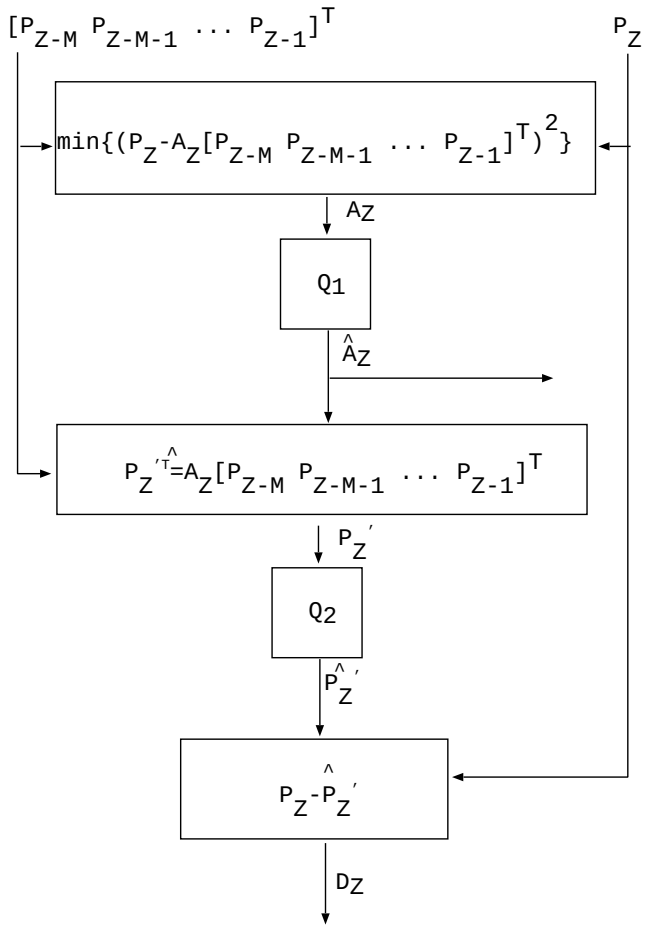

Fig 1. Spectral linear prediction.

4 Experimental Results

Figure 2 shows a stacked area plot of the overall contributions of the residual and side information as the function of the prediction length (M). In figure 3 a similar area plot shows compression ratios. The optimal value for M was determined to be 32. Figure 4 depicts the compression and decompression times for different values of M.

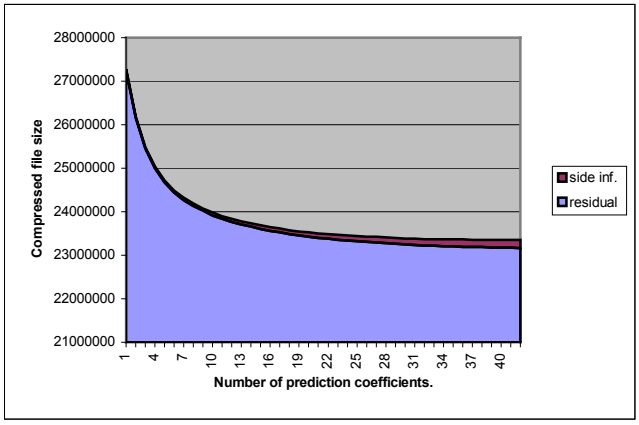

Fig. 2. Compressed file size as a function of the coefficients of linear prediction.

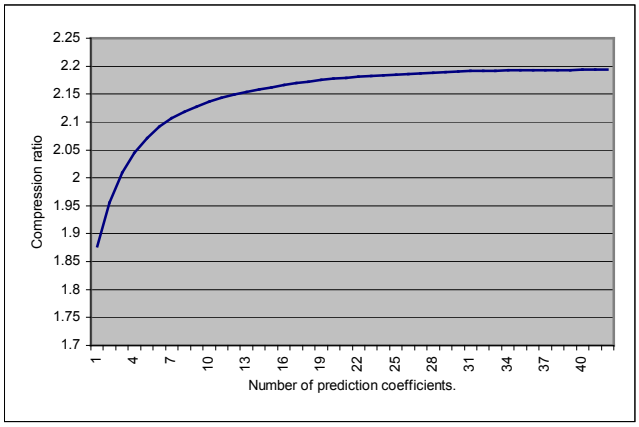

Fig. 3. Compression ratio as a function of the coefficients of linear prediction.

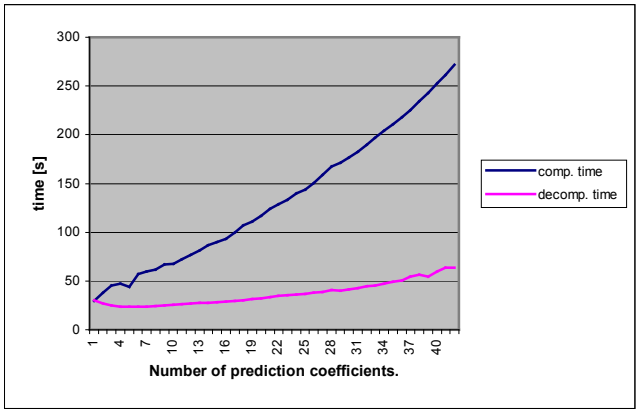

Fig. 4. Compression and decompression times as functions of the coefficients of linear prediction.

The compression ratios for proposed linear prediction method has been compared to compression ratios obtained with CALIC and JPEG-LS algorithms with FNNR [13] in Table 1 and adaptive linear prediction using optimal band ordering [20]. The band ordering is unnecessary for our method, since we are using so many bands in our spectral prediction scheme.

Table 1. Compression ratios for various compression schemes for the 10 tested granules.

Gran. №.	**CALIC + FNNR**	**JPEG-LS + FFNR**	**Adaptive Lin. Pred. + opt. Band ordering**	**Spectral linear pred.**
9	1.952	2.032	2.205	2.266
16	1.864	1.962	2.128	2.208
60	1.831	1.954	2.072	2.160
82	1.877	1.962	2.123	2.195
120	1.843	1.934	2.039	2.092
126	1.867	1.978	2.180	2.265
129	1.898	1.971	2.082	2.130
151	1.972	2.033	2.198	2.264
182	1.815	1.935	2.031	2.120
193	1.868	1.979	2.167	2.232
average	1.879	1.974	2.123	2.193

Judging from the results, it is obvious that the proposed spectral linear prediction method works better than CALIC and JPEG-LS. Our method produced 17 % and 11 % higher compression ratios than CALIC and JPEG-LS with FNNR, respectively. Compared to adaptive linear prediction method the improvement is 3 %.

Figure 5 compares entropies of the original and residual bands for granule 9. The entropy of the original bands is lower for 127 bands between bands 230 and 540. That justifies the use of the entropy coding without prediction for the selected bands.

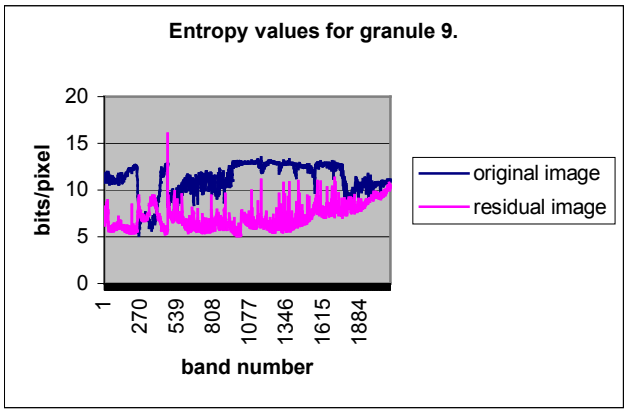

Fig. 5. Entropies of the original and residual bands for granule 9.

5 Conclusions

Spectral linear prediction method for lossless compression of 3D sounding images is proposed in this paper. On the whole, we based our prediction method on the assumption that since spectral correlation is much stronger than spatial correlation; prediction should be done only in the spectral direction. Otherwise, by adding a spatial predictor, we would combine a weaker predictor with a much better one. The results from that would be a much lower compression ratio. Since our prediction method outperforms the previous methods, our assumption seems to be correct.

The spectral linear prediction method is responsible for the best compression ratios known today for hyperspectral sounder images. The spectral prediction procedure is rather time consuming and for this reason, future research will concentrate on a research to achieve the same compression ratios at lower computational cost.

References:

[1] Sayood K., Introduction to Data Compression, University of Nebraska-Lincoln, Morgan Kaufmann Publishers, Academic Press, USA, 2000

[2] National Ocean and Atmospheric Administration. [Online]. Available: http://www.noaa.gov/, cited 1.6.2004.

[3] National Aeronautics and Space Administration (NASA). [Online]. Available: http://www-airs.jpl.nasa.gov, cited 1.6.2004.

[4] Aumann H.H. and Strow L., AIRS, The First Hyperspectral Infrared Sounder for Operational Weather Forecasting, *in Proc. of IEEE Aerospace Conference*, 2001, pp. 1683-1692.

[5] Bloom H.J., The Cross-track Infrared Sounder (CrIS): a Sensor For Operational Meteorological Remote Sensing, *in Proc. of the International Geosciences and Remote Sensing Symposium*, 2001, pp. 1341-1343.

[6] Phulpin T., Cayla F., Chalon G., Diebel D., and Schlüssel D., IASI Onboard Metop, *in Proc. of the 12th International TOVS Study Conference,* 2002.

[7] Smith W.L., Harrison F.W., Hinton D.E., Revercomb H.E., Bingham G.E., Petersen R., and Dodge J.C., GIFTS - The Precursor Geostationary Satellite Component of the Future Earth Observing System, *in Proc. of the International Geoscience and Remote Sensing Symposium*, 2002, pp. 357-361.

[8] Huang B., Huang H.L., Chen H., Ahuja A., Baggett K., Smith T.J., Heymann R.W., Data Compression Studies for NOAA Hyperspectral Environmental Suite (HES) using 3D Integer Wavelet Transforms with 3D Set Partitioning in Hierarchical Trees, *in Proc. of the SPIE International Symposium on Remote Sensing*, 2003.

[9] Jet Population Laboratory. [Online]. Available: http://aviris.jpl.nasa.gov/ .

[10] Weinberger M., Seroussi G, Sapiro G., The LOCO-I Lossless Image Compression Algorithm: Principles and Standardization into JPEG-LS, *Hewlett-Packard Laboratories Technical Report No. HPL-98-193R1*, 1998-1999.

[11] Wu X. and Memon N., Context-based, adaptive, lossless image coding, in *IEEE Trans. Commun.*, Vol. 45, pp. 437–444, Apr. 1997.

[12] S.Atek, T.Vladimirova. "A New Lossless Compression Method for Small Satellite On-Board Imaging" Proceeding of the 3rd WSEAS International Conference on Applied and Theoretical Mathematics, Miedzyzdroje, Poland, September 1-5, 2002, ed. N.E.Mastorakis, pp. 1871-1876, 2002.

[13] Huang B., Alok A, and Hung-Lung H., Improvements to Predictor-based Methods in Lossless Compression of 3D Hyperspectral Sounding Data via Higher Moment Statistics, *WSEAS Transactions on Electronics,* Vol. 1, No. 2, 2004

[14] Kubasova O., Toivanen P., Lossless Compression Methods for Hyperspectral Images, accepted for publication *in Proc. of 17th International Conference on Pattern Recognition*.

[15] Bormin H., Hung-Lung H., Alok A., and Hao C., Lossless Data Compression for Infrared Hyperspectral Sounders – An Overview, *in Proc. of 20th nternational Conference on Interactive Information and Processing Systems (IIPS) for Meteorology, Oceanography, and Hydrology*, 2004.

[16] AIRS date anonymous ftp, Available: ftp://ftp.ssec.wisc.edu/pub/bormin/HES, cited 1.6.2004
[17] S. Rouabhi, D.Fournier-Prunaret, Study of the DPCM Transmission System with a Periodic Input, 3th WSEAS CSCC (WSEAS International Multiconference on Circuits, Systems, Communications and Computers), Athens, Greece, July 4-9, 1999.
[18] G. N. Martin, Range encoding: an algorithm for removing redundancy from a digitalized image, in *Proc. of Video and Data Compression Conference,* 1979.
[19] M. Lundqvist's implementation of the range coder. [Online]. Available: http://w1.515.telia.com/~u51507446/, cited 1.6.2004.
[20] O. Kubasova, P. Toivanen, and J. Mielikäinen: Lossless Compression of 3D Hyperspectral Sounding Data via Statistical Image Characteristics, accepted for publication in *Proceedings of the 8th International WSEAS Conference on Systems: Special Symposium: 2nd International WSEAS Conference on Multidimensional Systems (MDS 2004)*, Athens, Greece, July 12-15, 2004.